ELSEVIER

Ceramics International 25 (1999) 1–6

CERAMICS INTERNATIONAL

# Microstructure and electric properties of a $SnO_2$ based varistor

S.A. Pianaro [a,*], P.R. Bueno [b], E. Longo [b], J.A. Varela [c]

[a] *Departamento de Engenharia de Materiais, UEPG, 84031-510, Ponta Grossa, PR, Brazil*
[b] *Departamento de Química, Universidade Federal de São Carlos, PO Box 676, 13565-905, São Carlos, SP, Brazil*
[c] *Instituto de Química, Universidade Estadual Paulista, PO Box 355, 14801-970 Araraquara SP, Brazil*

Received 10 May 1997; accepted 2 September 1997

**Abstract**

High non-linear $J \times E$ electrical characteristic ($\alpha = 41$) were obtained in the $Nb_2O_5$ and $Cr_2O_3$ doped CoO highly densified $SnO_2$ ceramics. X-ray diffraction analysis showed that these ceramics are apparently single phase. Electrical properties and microstructure are highly dependent on the $Cr_2O_3$ concentration and on the sintering temperature. Excess of $Cr_2O_3$ leads to porous ceramics destroying the material's electrical characteristics probably due to precipitation of second phase of $CoCr_2O_4$. Dopant segregation and/or solid solution formation at the grain boundaries can be responsible for the formation of the electrical barriers which originate the varistor behaviour. 

## 1. Introduction

The current density ($J$) and the applied electrical fields ($E$) of non-ohmic ceramic materials are related by the following relationship:

$$J = C.E^{\alpha} \tag{1}$$

where $\alpha$ is the non-linear coefficient and $C$ is a constant that is related with the microstructure. The non-linear coefficient is conventionally obtained for current densities around $1\,mA\,cm^{-2}$ [1]. In that current density the electrical breakdown field can be calculated through the relationship:

$$E_r = \frac{v_b}{\bar{d}} \tag{2}$$

with $v_b$ the barrier voltage and $\bar{d}$ the average grain size. For electrical field higher than $E_r$ the electrical conduction starts to be highly non-linear [2].

The first known ceramic material showing that property is the silicon carbide (SiC). This ceramic material consists of SiC particles (ranging from 50 to 100 μm in size), intimately bonded to a silica rich vitreous matrix [3]. Single phase BeO doped SiC varistors was developed by hot isostatic pressing [4]. Despite having superior electrical resistance than multiphase SiC varistors, the ceramic's non-linear coefficient remained low ($\alpha = 5$). High non-linear varistor materials ($\alpha = 50$) were developed by Matsuoka [1]. Those ceramics have complex chemical composition constituted by ZnO as major component, and small amounts of $Bi_2O_3$, $Sb_2O_3$, CoO, $MnO_2$ and $Cr_2O_3$. Their microstructure is multiphase being formed by ZnO grains as predominant phase and many other phases like the spinel ($Zn_7Sb_2O_{12}$), pyrochlore ($Zn_2Bi_3Sb_3O_{14}$) and several polymorphic phases of bismuth oxide ($\alpha,\beta,\delta$–$Bi_2O_3$), distributed in the structure. Those phases can be present in different proportions in the microstructure, depending on the heating and cooling rates used. Moreover, they can solubilize in different proportions as cobalt, manganese, chrome and antimony oxides [5–8]. Other known varistor systems are based in composite materials of a semiconductor (SiC), a conductive (a nickel compound), an insulator (vaporised SiC) and a binder (rubber). The non-linear coefficient of this material can range from 7.9 to 11.7 and the breakdown voltage ranges from 2.2 to $8.3\,KV\,cm^{-1}$, depending on the metal/semiconductor

* Corresponding author.

0272-8842/98/$—see front matter 
PII: S0272-8842(97)00076-X

rate in the chemical composition [9]. $TiO_2$-based varistor system doped with tantalum, niobium, barium, strontium and calcium oxides developed for relatively low voltage applications (1 to 20 Volts), with non-linear coefficient ranging from 3 to 7 [10]. Recently barium and bismuth oxide doped $TiO_2$ varistors were developed with better electrical properties [11]. Those varistors were classified as being multiphase due to the existence of small quantities of $BaTi_4O_9$ and $BiTi_2O_7$ phases located in the grain boundaries of the $TiO_2$ matrix. The best non-linear coefficient obtained for this system was 9.5 for a system with a grain boundary breakdown voltage of 0.8 V.

In former work [12] we described a $SnO_2$ based system, similar to the multicomponent ZnO varistor, constituted by $SnO_2.CoO.Nb_2O_5.Cr_2O_3$. In the present work microstructural and electrical modifications in those materials is presented according to variations on chemical composition and sintering temperature.

## 2. Experimental procedure

Analytical grades of $SnO_2$ (Merk), CoO (Riedel), $Nb_2O_5$ (Aldrich) and $Cr_2O_3$ (Vetec) were used in this work. The oxides were ball mill mixed in alcohol media with the following composition (in mole %): $(98.95-x)$ $SnO_2 + 1.00$ $CoO + 0.05$ $Nb_2O_5 + x$ $Cr_2O_3$, with $x$ ranging from 0.05 to 0.5 mole%. The resulted powders were uniaxial dry pressed (10 MPa) in cylindrical shape ($10.5 \times 1.0$ mm) and isostatically pressed at 210 MPa. The samples were sintered in a box furnace (Lindberg) at 1300 and 1350°C for 1 h, and slowly cooled down to the room temperature. The ceramic samples were thermally etched at 1290°C during 5 min and the scanning electron microscope (SEM, JEOL JSM - T330A) were used for microstructural analysis. Ceramic crystalline phases were determined by X-ray diffraction (SIEMENS D-500). Current-voltage electrical characteristics were determined by using a stabilized voltage source (Tectrol TCH 3000-2) along with two digital multimeters (Fluke 8050 A). The non-linear coefficient values ($\alpha$) were obtained by linear regression of the log-scale plot of current density vs applied electrical field in the region around 1 mA $cm^{-2}$ and the breakdown electrical fields were obtained at this current density. Grain sizes were determined by using SEM micrographs and the equation proposed by Mendelson [13].

## 3. Results and discussion

Current density vs electrical field curves for the $SnO_2$ based ceramic containing different concentration of $Cr_2O_3$ and sintered at 1300°C for 1h are shown in Fig. 1. A high degree of non-linearity was observed for the sample containing 0.05 mole% of $Cr_2O_3$. However varistor behaviour was not observed for samples sintered at the same temperature but with $Cr_2O_3$ concentration higher than 0.05 mole%.

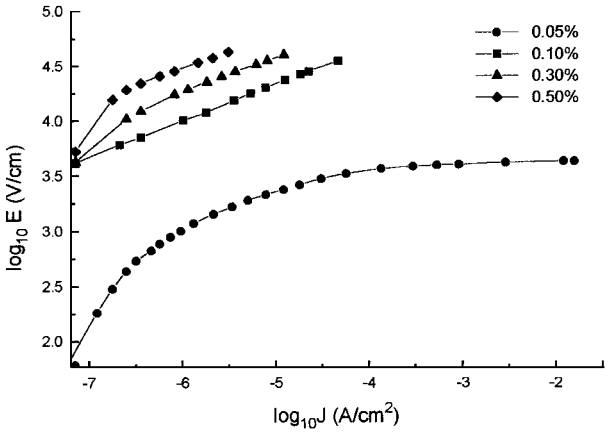


Fig. 1. Ln J vs ln E for the $SnO_2$ based varistor system sintered at 1300°C during 1 h with the composition (all in mole%) $(98.95-x)$ $SnO_2 + 1.00$ $CoO + 0.05$ $Nb_2O_5 + xCr_2O_3$ ($x$ ranging from 0.05 to 0.5 mole%).

Fig. 2 shows current density vs applied electrical field for samples with the same composition but sintered at 1350°C during 1 h. At this temperature varistor behaviour was observed for samples containing 0.05 and 0.10 mole% $Cr_2O_3$. Ceramic samples containing 0.3 mole% of $Cr_2O_3$ and sintered at this temperature exhibited a non-linear behaviour at low current densities before assuming a linear behaviour, which is an indicative of a high electrical resistance inside the grains that leads to early initialisation of the post-failure region [14]. For $Cr_2O_3$ concentrations higher than 0.5 mole% the characteristic electric curves are linear. Parameters $\alpha$ and $E_r$ obtained from the current density vs applied

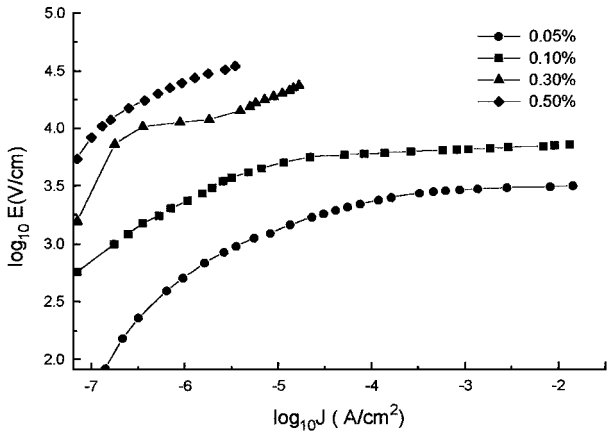


Fig. 2. Ln J vs ln E for the $SnO_2$ based varistor system sintered at 1350°C during 1 h with the composition (all in mole%) $(98.95-x)$ $SnO_2 + 1.00$ $CoO + 0.05$ $Nb_2O_5 + xCr_2O_3$ ($x$ ranging from 0.05 to 0.5 mole%).

electric field curves, as well as the grain size and voltage barrier are displayed in Table 1.

Analysing the results of Table 1 and Figs. 1 and 2 it is observed that the electrical properties of $SnO_2$ based ceramics are deeply dependent on the $Cr_2O_3$ concentration and on the sintering temperature. $SnO_2$ based ceramic samples containing 0.05 mole% of $Cr_2O_3$ and sintered at 1300°C displayed a high non-linear coefficient ($\alpha = 41$) which is very close to those of traditional ZnO varistors ($\alpha \cong 50$). The breakdown electrical field ($E_r$) in this sintering condition is 3990 V cm$^{-1}$. Increasing the sintering temperature for this same composition the non-linear coefficient drops to $\alpha = 35$ and the breakdown electrical field drops to 2900 V cm$^{-1}$. That reduction on the breakdown electrical field is related with the increase of the ceramic's grain size what, as expected, increase along with the sintering temperature. Then the number of effective electrical barriers decreases, since that the barrier voltage remained practically constant, according to Eq. (2).

For $SnO_2$ based ceramics containing 0.10 mole% $Cr_2O_3$ and sintered at 1350°C the non-linear behaviour decrease ($\alpha = 29$) associated to a high value of breakdown electrical field ($E_r = 6800$ V cm$^{-1}$). Compared with the $SnO_2$ based ceramic containing 0.05 mole% $Cr_2O_3$ and sintered at the same temperature a strong dependence between the breakdown electrical field and the $Cr_2O_3$ concentration is observed. As observed in Table 1 the grain size decrease from 7.5 to 5.0 μm when the $Cr_2O_3$ concentration increases from 0.05 to 0.10 mole%. This decrease in grain size is not sufficient to explain the large increase of the single grain boundary breakdown electrical field. Then, as observed in Table 1 the voltage barrier ($v_b$) is dependent on $Cr_2O_3$ concentration and increases from 2.2 to 3.4 volts/barrier when the concentration increases from 0.05 to 0.10 mole% in $SnO_2$ based ceramics sintered at 1350°C. This voltage barrier increase can be associated to the increase of the $Cr_2O_3$ concentration at the $SnO_2$ grain surface through creation of the atomic defect $Cr_{sn}$ or due to segregation of this oxide at grain boundary. The highest value of the single grain boundary breakdown voltage ($v_b$) for the $SnO_2$ varistor system (3.4 V) is essentially the $SnO_2$ band gap, and this supports models in which electrical nonlinearity is explained as a consequence of minority carrier creation [15]. This means that the number of effective voltage barrier increases with increasing concentration of $Cr_2O_3$ reaching the maximum value for 0.10 mole%.

Table 1
Non-linear coefficient values (α), breakdown electrical field ($E_r$), average grain size ($d$), and barrier voltage ($v_b$) for the system with the composition (all in mole%): (98.95−$x$) $SnO_2$ + 1.00 CoO + 0.05 $Nb_2O_5$ + $x$$Cr_2O_3$, sintered at 1300 and 1350°C during 1h

| | 1300°C | | | | 1350°C | | | |
|---|---|---|---|---|---|---|---|---|
| Molar % | α | $E_r$ (V/cm) | $d$ (μm) | $v_b$ (V/b) | α | $E_r$ (V/cm) | $d$ (μm) | $v_b$ (V/b) |
| 0.05 | 41 | 3990 | 5.4 | 2.2 | 35 | 2900 | 7.5 | 2.2 |
| 0.10 | – | – | 4.5 | – | 29 | 6800 | 5.0 | 3.4 |
| 0.30 | – | – | 3.1 | – | – | – | 3.4 | – |
| 0.50 | – | – | 2.4 | – | – | – | 3.0 | – |

In Fig. 3 the current density vs applied electric field curves measured at room temperature for $SnO_2$ based samples containing 0.05 mole% of $Cr_2O_3$ and sintered at 1300 and 1350°C are compared. In addition to lower non-linear coefficient obtained for samples sintered at 1350°C, the current leakage is higher. Considering that the voltage barrier ($v_b$) remains essentially the same for both sintering temperatures, the increase of current leakage can be associated to the reduction of the average number of barriers since that the grain size increases from 5.4 to 7.5 μm.

X-ray diffraction spectra of $SnO_2$ based samples with different $Cr_2O_3$ compositions and sintered at 1300°C are displayed in Fig. 4. It is observed in this figure that, independent of the $Cr_2O_3$ concentration, no other crystalline phase besides cassiterite ($SnO_2$) is observed indicating that the system is single phase within the detection precision of the X-ray diffraction. The same trend is observed for samples sintered at 1350°C.

The addition of 1.0 mole% of CoO to $SnO_2$ ceramics promotes densification as high as 98.5% of theoretical density when sintered at 1300°C during 1 h. However, the addition of 0.05 mole% to that ceramics lowers the density to 96.3% of theoretical density when sintered in the same condition [15]. Moreover, the addition of $Cr_2O_3$ to the $SnO_2$ ceramic containing CoO and $Nb_2O_5$ modify the final density when this ceramic is sintered at 1300 and 1350°C as showed in Table 2. According to this table, additions of $Cr_2O_3$ up to concentration of 0.3 mole% do not change significantly the final density of $SnO_2$ based ceramic when sintered at 1300 or 1350°C. However, increasing the $Cr_2O_3$ concentration to

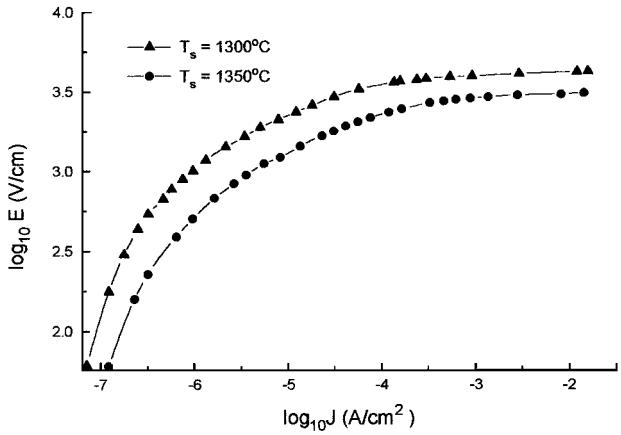


Fig. 3. Ln J vs ln E for the $SnO_2$ based varistor system with the composition (all in mole%) 98.90% $SnO_2$ + 1.00 CoO + 0.05 $Nb_2O_5$ + 0.05 $Cr_2O_3$, sintered at 1300 and 1350°C during 1 h.

0.5 mole% the final density of the ceramic decreases substantially when sintered in both temperatures. According to the results presented on Table 2 these variations cannot be associated to mass loss during sintering. For sintering of the $SnO_2$ based ceramic at 1300°C the mass loss decreases with increasing $Cr_2O_3$ concentration from 0.1 to 0.5 mole%. Increasing the sintering temperature to 1350°C the mass loss remain practically constant with increasing $Cr_2O_3$ concentration from 0.1 to 0.5 mole%.

Figs. 5 and 6 show the characteristic microstructures of the $SnO_2$ based ceramics sintered at 1300 and 1350°C, respectively. These figures clearly show the effect of $Cr_2O_3$ concentration on the microstructure of $SnO_2$ based ceramics. Increasing $Cr_2O_3$ concentration leads to microstructure with decreasing grain size for both sintering temperatures. The decrease in grain size could be associated to precipitations of secondary phases in the grain boundaries as it occurs during sintering of ZnO varistors with the formation of spinel phase [16]. No secondary phase precipitated at grain boundaries was observed by X-ray diffraction or by SEM observations. However it was formally observed by high resolution TEM that small amount of $CoSnO_4$ phase precipitates from solid state at grain boundaries when the $SnO_2$ ceramics containing 1.0 mole% CoO is sintered at 1300°C [17]. Whenever the $Cr_2O_3$ forms a secondary phase with CoO or $SnO_2$ is not well understood yet in this ceramic. However there is a possibility of formation of $CoCr2O_4$ phase that could precipitate at grain boundaries. If this occurs, the decrease in the final

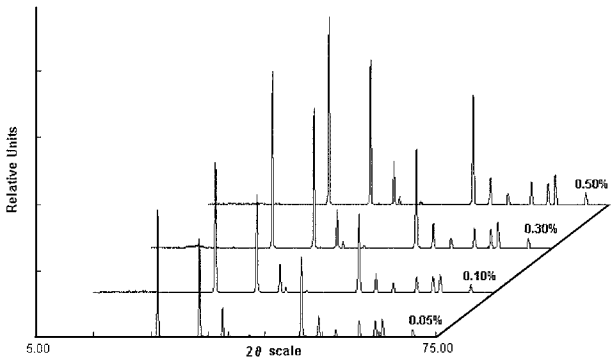


Fig. 4. X-ray diffraction spectra for the $SnO_2$ based varistor sintered at 1300°C during 1 h with the composition (all in mole%) $(98.95-x)$ $SnO_2 + 1.00$ $CoO + 0.05$ $Nb_2O_5 + xCr_2O_3$ ($x$ ranging from 0.05 to 0.5 mole%).

Table 2
Relative densities variation with $Cr_2O_3$ composition for the system with the composition (all in mole%): $(98.95-x)$ $SnO_2 + 1.00$ $CoO + 0.05$ $Nb_2O_5 + xCr_2O_3$ sintered at 1300 and 1350°C during 1h

| | 1300°C | | | 1350°C | | |
|---|---|---|---|---|---|---|
| Molar % | ρ ($g\,cm^{-3}$) | ρT (%) | Wt loss (%) | ρ ($g\,cm^{-3}$) | ρT (%) | Wt loss (%) |
| 0.05 | 6.37 | 91.7 | 1.19 | 6.36 | 91.5 | 1.13 |
| 0.10 | 6.38 | 91.8 | 1.02 | 6.49 | 93.4 | 1.13 |
| 0.30 | 6.36 | 91.5 | 0.99 | 6.43 | 92.5 | 1.04 |
| 0.50 | 6.03 | 86.8 | 0.89 | 6.00 | 86.3 | 1.04 |

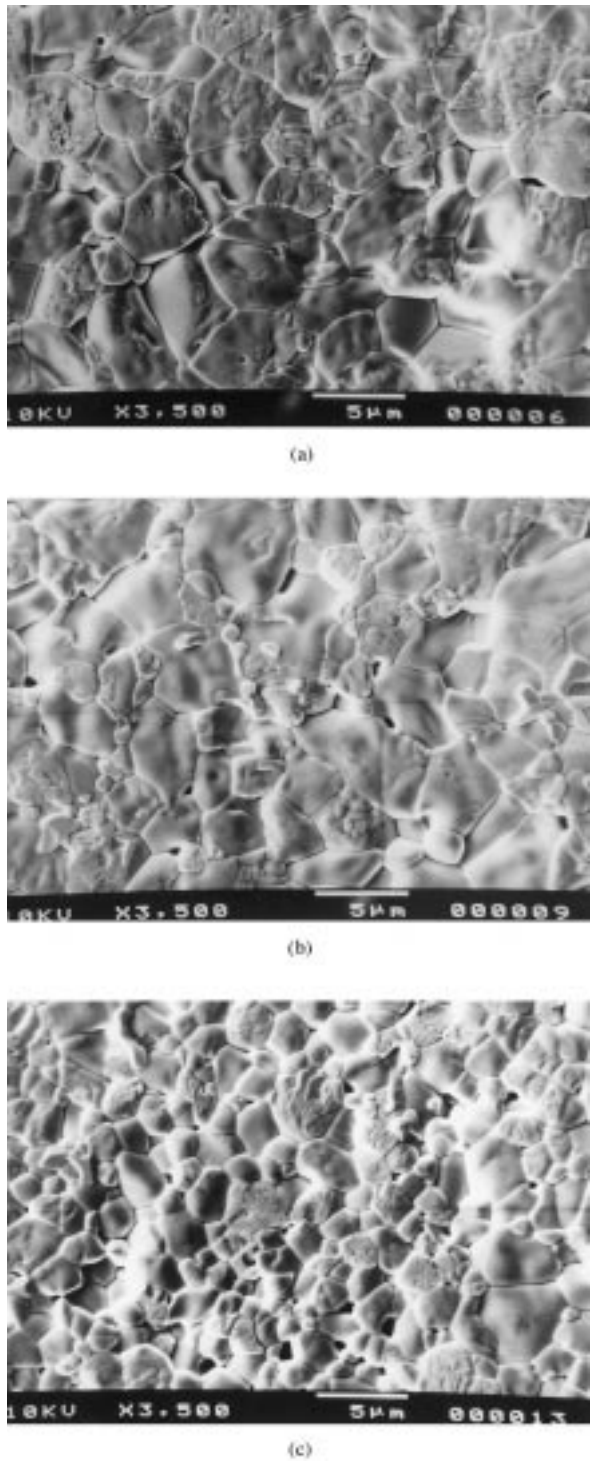


Fig. 5. Microstructure variation of the $SnO_2$ varistor system sintered at 1300°C during 1 h with the composition (all in mole%) $(98.95-x)$ $SnO_2 + 1.00$ $CoO + 0.05$ $Nb_2O_5 + xCr_2O_3$: (a) $x = 0.05$; (b) $x = 0.10$; and (c) $x = 0.30$.

density of $SnO_2$ based ceramics could be associated to the decrease of oxygen vacancy formation in the grain boundary due to reaction of cobalt ions with the $Cr_2O_3$ forming $CoCr_2O_4$. In this case the sintering and grain growth rate would decrease with increasing amount of $Cr_2O_3$ as observed in this study (Figs. 5 and 6). Considering that the formation of electrical barriers essentials for the varistor behaviour is prevented by porosity and that the sintered density of $SnO_2$ based ceramic decrease for $Cr_2O_3$ concentrations above 0.3 mole%, it is expected that the varistor behaviour of $SnO_2$ ceramics decreases with higher concentration of $Cr_2O_3$. Lower concentration of $Cr_2O_3$ favour microstructure development since that does not affect the mass transport for sintering as well as favours the oxygen adsorption at grain boundaries increasing the varistor behaviour.

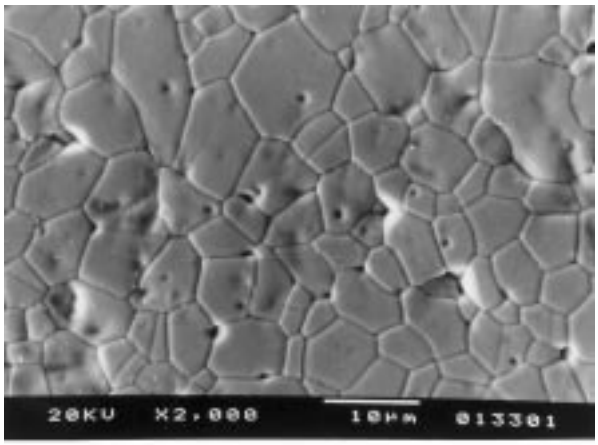


(a)

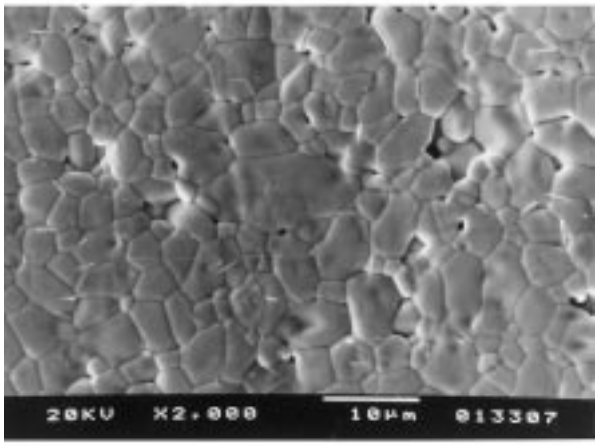


(b)

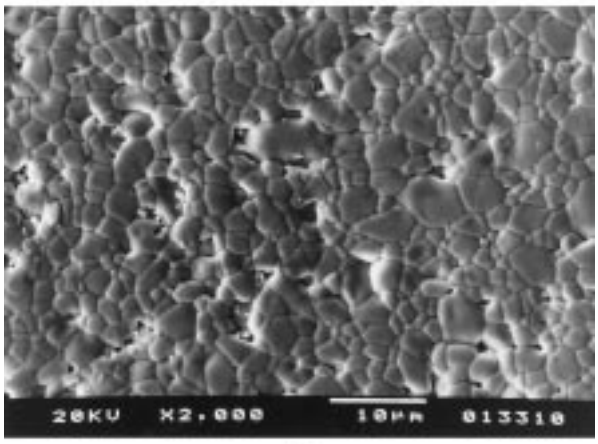


(c)

Fig. 6. Microstructure variation of the $SnO_2$ varistor system sintered at 1350°C during 1 h with the composition (all in mole%) $(98.95-x)$ $SnO_2 + 1.00$ $CoO + 0.05$ $Nb_2O_5 + xCr_2O_3$: (a) $x = 0.05$; (b) $x = 0.10$; and (c) $x = 0.30$.

Considering the high non-linear behaviour of the $SnO_2$ based ceramics it is opportune compare with the well-known multicomponent ZnO varistor systems that show great non-ohmic characteristic. Characteristic curves of the two varistor systems one being the ZnO based varistor, studied in a former work [18] and other the $SnO_2$ based varistor reason of this study are depict in Fig. 7. Table 3 shows data of non-linear coefficient ($\alpha$) and the breakdown electrical field ($E_r$) extracted from its respective characteristic curves, along with their compositions and microstructure details. The electrical behaviour of these two systems are very similar as observed in the displayed characteristic curves of Fig. 7. The non-linear coefficient values are almost the same for the two systems ($\alpha = 41$ for the $SnO_2$ based varistor and $\alpha = 42$ for the ZnO based varistor). However, there are significant differences in the electrical breakdown field value, as $SnO_2$ based varistor showed superior value than the ZnO based varistor. ZnO based varistor showed also lower current leakage, indicating a higher electrical resistance of the grain boundary.

The most remarkable difference in those systems is the clear difference in microstructure aspects of both

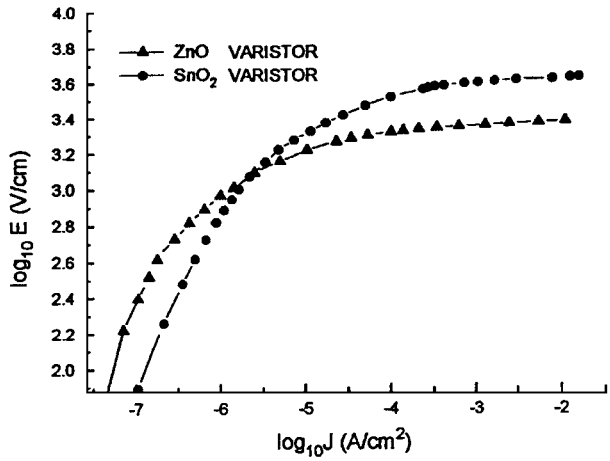


Fig. 7. Ln J vs ln E characteristic curves for $SnO_2$ and ZnO based varistors at 28°C. Varistors with the following composition (all in mole%): (a) 98.90 $SnO_2 + 1.00$ $CoO + 0.05$ $Nb_2O_5 + 0.05$ $Cr_2O_3$; (b) 94.9% $ZnO + 0.5\%$ $Bi_2O_3 + 1.5\%$ $CoO + 1.5\%$ $Sb_2O_3 + 1.5\%$ $MnO_2 + 0.1\%$ $Cr_2O_3$.

Table 3
Comparison of chemical composition, electrical properties and microstructure aspects of ZnO and $SnO_2$ based varistors

| Chemical Composition | $T_s$ (°C) | $d$ (μm) | Phases | α | $E_r$ (V/cm) |
|---|---|---|---|---|---|
| 98.9% $SnO_2$ + 1.0% CoO + 0.05% $Nb_2O_5$ + 0.05% $Cr_2O_3$ | 1300 | 5.4 | $SnO_2$ | 41 | 3990 |
| 94.9% ZnO + 0.5% $Bi_2O_3$ + 1.5% $Sb_2O_5$ + 1.5% CoO + 1.5% $MnO_2$ + 0.1% $Cr_2O_3$ | 1250 | 10.0 | ZnO + β-$Bi_2O_3$ + α-$Zn_7Sb_2O_{12}$ + $Zn_2Bi_3Sb_3O_{14}$ | 42 | 2290 |

varistor systems. ZnO varistor system is a multiphase one being the ZnO grains as predominant phase and several secondary phases as the spinel phase ($Zn_7Sb_2O_{12}$), pyrochlore phase ($Zn_2Bi_3Sb_3O_{14}$) and a polymorphic phase of bismuth oxide. The ZnO varistor microstructure formation is very complex, going to liquid phase formation and precipitation of several phases in the material microstructure. Those phases play important role in the formation of the varistor microstructure and, consequently, in its electrical properties [19]. Otherwise $SnO_2$ based varistors are apparently single phase and its microstructure development occurs by solid state sintering. This means that dopant solid solution or/and solid state phase precipitation at grain boundaries controls the varistor electrical properties. Moreover the amount of secondary phase formed by solid state precipitation at grain boundaries, if occurs, is too low to affects significantly the electrical properties degradation. For this reason the processing conditions for $SnO_2$ based varistors such as, heating and cooling rates, are not so critical parameters making an easier sintering process. The relatively simple chemical composition of the $SnO_2$ based varistor compared with ZnO based varistor also should be noticed. The application of ZnO based varistors is restricted by its easy degradation face to chemically aggressive environments, as the zinc oxide is easily attacked by weak acid or alkaline environments [6,20]. Otherwise, $SnO_2$ is chemically non reactive and thus can be used in aggressive environments, without easy chemical degradation. For example, $SnO_2$ ceramics is used as conductive fusion electrodes for making special glasses, once this oxide is resistant to glass attack which is done at high temperatures [3]. Then the new $SnO_2$ based varistor can be a very attractive alternative to ZnO based varistors. However, nothing is known about electrical degradation of this system. This study is still being conducted in our laboratory and it is going to be presented in near future.

## 4. Conclusion

Highly non-linear electrical properties were obtained for high densified $SnO_2$ ceramics. Contrary to ZnO varistors, these new ceramic materials are obtained by solid state sintering and the amount of possible secondary phase precipitated at grain boundary, if exist, is very small. Being this way their electrical properties are closely related to dopant solid solution formation and/or solid state precipitation of a new phase at the grain boundary. Then the electrical barrier to electronic transport is created leading to high non-ohmic character. The ceramic microstructure is strongly dependent on the $Cr_2O_3$ concentration and on the sintering temperature. This oxide form solid solution segregated at grain boundaries and could react with CoO, also segregated at grain boundary, precipitating as $CoCr_2O_4$ in the grain boundary and could control the sintering and grain growth rates. Thus, excess of it in the chemical composition leads to formation of porous microstructure that is deleterious for varistor behaviour. Otherwise small additions of this oxide create extremely favorable microstructure for non-ohmic conduction.

## References

[1] M. Matsuoka, Jpn. J. Appl. Phys. 10 (1971) 736.
[2] L.M. Levinson, H.R. Philipp, Ceram. Bull., 65 (1986) 639.
[3] A.J. Moulson, J.M. Herbert, Electroceramics. Chapman and Hall, New York, 1990, pp. 123, 135.
[4] K. Maeda, T. Miyoshi, Y. Takeda, K. Nakamura, S. Ogihara, M. Ura, Advances, Ceramics, vol 7 in: M.F. Yan, A.H. Heur (Eds.), American Ceramic Society, Columbus OH, 1983, p. 260.
[5] G.J. Wong, J. Appl. Phys. 46 (1975) 1654.
[6] A.T. Santhanam, T.K. Gupta, W.G. Carlson, J. Appl. Phys. 50 (1979) 852.
[7] M. Inada, Jpn. J. Appl. Phys., 19 (1980) 409.
[8] E. Olsson, G. Dunlop, R. Osterlund, J. Am. Ceram. Soc. 76 (1993) 145.
[9] F.A. Modine, J. Appl. Phys. 64 (1988) 4229.
[10] M.F. Yan, W.W. Rhodes, Appl. Phys. Lett. 40 (1982) 536.
[11] S.L. Yang, J.M. Wu, J. Am. Ceram. Soc. 76 (1993) 145.
[12] S.A. Pianaro, P.R. Bueno, E. Longo, J.A. Varela, J. Mater. Sci. Lett. 14 (1995) 692.
[13] M.I. Mendelson, J. Am. Ceram. Soc., 52 (1969) 443.
[14] L.M. Levinson, H.R. Phillip, J. Appl. Phys. 47 (1976) 3116.
[15] S.A. Pianaro, P.R. Bueno, P. Olivi, E. Longo, J.A. Varela, J. A., submitted.
[16] T. Kimura, H. Kajiyama, J. Kim, T. Yamagushi, J. Am. Ceram. Soc., 72 (1989) 140.
[17] J.A. Varela, J.A. Cerri, E.R. Leite, E. Longo, M. Shansuzzoha, R.C. Bradt, Ceram. Int., in press.
[18] S.A. Pianaro, Thesis, Ms., Federal University of Sao Carlos, 1990.
[19] M. Inada, Jpn. J. Appl. Phys., 17 (1978) 673.
[20] M. Inada, Jpn. J. Appl. Phys., 18 (1979) 1439.